

NUMERICAL ASPECTS OF WAVE PROPAGATION IN A BIOT MEDIUM

Fabio I. Zyserman^a and Juan E. Santos^{a,b}

^aCONICET, Fac. de Cs. Astronómicas y Geofísicas, UNLP, Paseo del Bosque s/n, 1900 - La Plata,
Argentina

^bDepartment of Mathematics, Purdue University, 150 N. University Street, W. Lafayette, IN,
47907-2067, USA

Keywords: Dispersion Analysis, Biot equation, Finite elements.

Abstract. Biot's equations appear in geophysical applications where wave propagation in fluid saturated porous media is considered, although in recent years they have also been applied to model ultrasonic technics for osteoporosis or other bone-modifying diseases diagnosis.

It is well known that finite element solutions for propagating waves deteriorate rapidly with increasing dimensionless wavenumber, even when the number of elements per wavelength is kept constant; this is referred to as *pollution error*.

In this work we present a detailed analysis of the numerical behaviour of a finite element method used to approximate the solution of the 1D Biot equations.

The study is performed by deriving the dispersion relations and by evaluating the derived quantities, such as the dimensionless phase and group velocities.

1 INTRODUCTION

The propagation of waves in a porous elastic solid saturated by a single-phase compressible viscous fluid was first analyzed by Biot in several classic papers. Biot assumed that the fluid may flow relative to the solid frame causing friction. In the low frequency range, such flow is of laminar type and obeys Darcy's law for fluid flow in porous media. In the high frequency range, Biot pointed out that a frequency correction factor had to be introduced in the Darcy coefficient. Biot predicted the existence of two compressional waves, which he denoted type I and type II compressional waves, and one shear wave. The three waves suffer attenuation and dispersion in certain ranges of frequencies. The type I and shear waves have a behaviour similar to that in an elastic solid, with high phase velocities, low attenuation and very little dispersion. The type II wave behaves as a diffusion-type wave due to its low phase velocity and very high attenuation and dispersion. For shortness, a porous elastic solid saturated by a single-phase fluid will be referred to as a Biot medium.

The purpose of this paper is to analyze the numerical dispersion associated with the numerical solution of the one dimensional Biot's equations of motion employing the finite element methods as described in what follows.

Following the methods introduced in (Zyserman et al., 2003) we analyze the numerical behaviour of the finite element approximation by finding the analytic and numerical dispersion relations, and studying the numeric phase and group velocities, and wave attenuation. We investigate how the defined numerical quantities depend on the number of points per wavelength, so as to give an estimated lower bound on the latter in order to get a desired accuracy.

2 REVIEW OF BIOT'S THEORY

We consider a one dimensional porous solid saturated by a single phase, compressible viscous and assume that the whole aggregate is isotropic. Let u^s and \tilde{u}^f denote the averaged displacements of the solid and fluid phases, respectively; then

$$u^f = \phi(\tilde{u}^f - u^s),$$

is the average relative fluid displacement per unit volume of bulk material, where ϕ denotes the solid effective porosity. Following (Biot, 1962), and denoting $u = (u^s, u^f)$, the 1D stress-strain relations can be written in the form:

$$\begin{aligned} \tau(u) &= 2\mu \frac{\partial u^s}{\partial x} + (\lambda_c \frac{\partial u^s}{\partial x} + D \frac{\partial u^f}{\partial x}), \\ p_f(u) &= -D \frac{\partial u^s}{\partial x} - K_{av} \frac{\partial u^f}{\partial x}. \end{aligned} \quad (1)$$

Here $\tau(u)$ is the stress tensor and $p_f(u)$ the fluid pressure. The coefficient μ is equal to the shear modulus of the bulk material, considered to be equal to the shear modulus of the dry matrix. Also $\lambda_c = K_c - 2\mu$, with K_c being the bulk modulus of the saturated material. Following (Santos et al., 1992), (Gassmann, 1951) the coefficients in (1) can be obtained from the relations

$$\begin{aligned} \alpha &= 1 - \frac{K_m}{K_s}, & K_{av} &= \left[\frac{\alpha - \phi}{K_s} + \frac{\phi}{K_f} \right]^{-1} \\ K_c &= K_m + \alpha^2 K_{av}, & D &= \alpha K_{av}, \end{aligned} \quad (2)$$

where K_s , K_m and K_f denote the bulk modulus of the solid grains composing the solid matrix, the dry matrix and the saturant fluid, respectively. The coefficient α is known as the effective stress coefficient of the bulk material.

2.1 The equations of motion

Let ρ_s and ρ_f denote the mass densities of the solid grains and the fluid and consider

$$\rho_b = (1 - \phi)\rho_s + \phi\rho_f$$

to be the mass density of the bulk material. Then the equations of motion are (Santos et al., 1992)

$$\begin{aligned} \rho_b \frac{\partial^2 u^s}{\partial t^2} + \rho_f \frac{\partial^2 u^f}{\partial t^2} - \frac{\partial \tau(u)}{\partial x} &= f^s, \\ \rho_f \frac{\partial^2 u^s}{\partial t^2} + g \frac{\partial^2 u^f}{\partial t^2} + b \frac{\partial u^f}{\partial t} + \frac{\partial p_f(u)}{\partial x} &= f^f. \end{aligned} \quad (3)$$

The mass coupling coefficient g represents the inertial effects associated with dynamic interactions between the solid and fluid phases, while the coefficient b includes the viscous coupling effects between such phases. They are given by the relations

$$b = \frac{\eta}{k}, \quad g = \frac{S\rho_f}{\phi}, \quad S = \frac{1}{2} \left(1 + \frac{1}{\phi} \right), \quad (4)$$

where η is the fluid viscosity and k the absolute permeability. S is known as the structure or tortuosity factor. Above a certain critical frequency ω_c the coefficients b and g become frequency dependent (Biot, 1956b; Johnston et al., 1987; Carcione, 2001); this effect is associated with the departure of the flow from the laminar Poiseuille type at the pore scale. The value of ω_c can be estimated by the formula

$$\omega_c = \frac{2\eta\phi}{a_p^2\rho_f}, \quad (5)$$

where $a_p = 2(5k/\phi)^{1/2}$ is the effective flow channel or pore size parameter calculated in terms of the permeability k and the porosity ϕ (Johnson, 1982; Bear, 1972; Scheidegger, 1974; Hovem and Ingram, 1979).

In this paper frequencies below ω_c are considered, so that the mass coupling and viscous coupling coefficients are assumed to be constant.

The equations (3) stated in the space-frequency domain become (Biot, 1956a), (Biot, 1956b), (Berryman, 1980):

$$-\omega^2\rho_b u^s - \omega^2\rho_f u^f - \frac{\partial \tau(u)}{\partial x} = f^s \quad (6)$$

$$-\omega^2\rho_f u^s - \omega^2 g u^f + i\omega b u^f + \frac{\partial p_f(u)}{\partial x} = f^f, \quad (7)$$

where $\omega = 2\pi f$ is the angular frequency. These equations can be rewritten as

$$-\omega^2 \mathcal{P}u + i\omega \mathcal{B}u - \mathcal{L}(u) = \mathcal{F}, \quad (8)$$

where

$$\mathcal{L}(u) = \left(\frac{\partial \tau(u)}{\partial x}, -\frac{\partial p_f(u)}{\partial x} \right),$$

$$\mathcal{P} = \begin{pmatrix} \rho_b & \rho_f \\ \rho_f & g \end{pmatrix}, \quad \mathcal{B} = \begin{pmatrix} 0 & 0 \\ 0 & b \end{pmatrix} \quad \text{and } \mathcal{F} = (f^s, f^f).$$

Naturally, boundary conditions must be provided in order to completely define this problem. If Γ is the boundary of the domain Ω , let ν the unit outer normal on Γ . Of course, as the 1D case is being considered, $\nu = 1$ or $\nu = -1$, and Γ is a set of two points. Set

$$\mathcal{G}_\Gamma(u) = \left(\tau(u)\nu \cdot \nu, p_f(u) \right), \tag{9a}$$

$$S_\Gamma(u) = (u^s \cdot \nu, u^f \cdot \nu). \tag{9b}$$

The proposed absorbing boundary condition reads

$$-\mathcal{G}_\Gamma(u) = i\omega \mathcal{D} S_\Gamma(u). \tag{10}$$

Here the matrix \mathcal{D} in (10) is positive definite; it can be obtained from $\mathcal{D} = \mathcal{P}^{\frac{1}{2}} \mathcal{N}^{\frac{1}{2}} \mathcal{P}^{\frac{1}{2}}$, where $\mathcal{N} = \mathcal{P}^{-\frac{1}{2}} \mathcal{M}^{\frac{1}{2}} \mathcal{P}^{-\frac{1}{2}}$ and

$$\mathcal{M} = \begin{pmatrix} \lambda_c + 2\mu & \alpha K_{av} \\ \alpha K_{av} & K_{av} \end{pmatrix}. \tag{11}$$

2.2 Phase velocities and attenuation

Consider a compressional plane wave traveling along the x -axis, and define the potentials

$$\varphi = A_c e^{i(\omega t - qx)}, \quad \psi = B_c e^{i(\omega t - qx)},$$

where

$$q = \text{1D complex wave vector} = q^r - iq^i. \tag{12}$$

Replacing $U = \frac{\partial \varphi}{\partial x}$ and $W = \frac{\partial \psi}{\partial x}$ in (8), and assuming $\mathcal{F} = 0$, the equations

$$\begin{aligned} (\rho\omega^2 - H_c q^2) A_c + (\rho_f \omega^2 - D q^2) B_c &= 0, \\ (\rho_f \omega^2 - D q^2) A_c + (g\omega^2 - i\omega b - M q^2) B_c &= 0. \end{aligned} \tag{13}$$

are obtained. The fact that the strain and kinetic energies are positive allow the choice of two physically meaningful roots q_1 and q_2 of q in (13) having negative imaginary part, corresponding to the P_1 (fast) and P_2 (slow) compressional waves, respectively.

The present study will be carried out considering phase velocities $v_j = \omega / |\text{Re}(q_j)|$ and attenuation q_j^i .

3 THE FINITE ELEMENT PROCEDURE

The variational formulation of equations (8)-(10) can be written, considering a domain $\Omega = (0, 1)$ as (see (Santos et al., 2005) for details):

$$\begin{aligned} -\omega^2 (\mathcal{P}u, v) + i\omega (\mathcal{B}u, v) + \mathcal{A}(u, v) + i\omega \langle \mathcal{D} S_\Gamma(u), S_\Gamma(v) \rangle &= (\mathcal{F}, v), \\ v = (v^s, v^f)^t \in \mathcal{V}, \end{aligned} \tag{14}$$

where the space \mathcal{V} is $H^1(\Omega)$; $\mathcal{A}(u, v)$ is the following bilinear form:

$$\mathcal{A}(u, v) = \left(\tau(u), \frac{\partial v^s}{\partial x} \right) - \left(p_f(u), \frac{\partial v^f}{\partial x} \right), \quad u, v \in \mathcal{V}, \quad (15)$$

and, as usual, (\cdot, \cdot) denotes the inner product in Ω and $\langle a, b \rangle \equiv f(0)g^*(0) + f(1)g^*(1)$ the inner product on the domain boundary Γ (* means complex conjugate).

Turning the attention to the discrete approximation of equation (14), let V^h be the space of C^0 piecewise linear functions used to approximate both the solid and fluid displacements, i.e.

$$V^h = \{v \in C^0(\Omega) | v|_{[x_{i-1}, x_i]} \in P_1, \quad i = 1, \dots, N\}. \quad (16)$$

The *global* finite element procedure is defined as follows: find $u^h = (u^{s,h}, u^{f,h}) \in V^h$ such that

$$\Theta_h(u^h, v) = (\mathcal{F}, v), \quad v = (v^s, v^f) \in V^h. \quad (17)$$

Here

$$\Theta_h(u^h, v) = -\omega^2 (\mathcal{P}u^h, v) + i\omega (\mathcal{B}u^h, v) + \mathcal{A}(u^h, v) + i\omega \langle \mathcal{D} S_\Gamma(u^h), S_\Gamma(v) \rangle. \quad (18)$$

4 NUMERICAL DISPERSION ANALYSIS

Consider writing the solutions to equations (13) in dimensionless form, for what the following dimensionless parameters are defined:

$$\delta_1 = \frac{\mu}{\mu + 2\lambda_c}, \quad \delta_2 = \frac{D}{\mu + 2\lambda_c}, \quad \delta_3 = \frac{M}{\mu + 2\lambda_c}, \quad (19)$$

$$(20)$$

$$\omega_c = \frac{b}{\phi\rho_f}, \quad \omega_a = \frac{\omega}{\omega_c}, \quad (21)$$

$$\gamma_1 = \frac{\rho_f}{\rho_b}, \quad \gamma_2 = \frac{g}{\rho_b}, \quad \gamma_3 = \frac{1}{\phi\gamma_1\omega_a}. \quad (22)$$

Introducing also a reference velocity $V_R = \sqrt{\frac{\lambda_c + 2\mu}{\rho_b}}$, the solutions to equations (13) can now be written as

$$\frac{V_R^2}{\omega_c^2} q^2 = \omega_a^2 \left(\frac{1}{2(-\delta_2^2 + \delta_3)} \left((\gamma_2 + i\gamma_3/\omega_a - 2\gamma_1\delta_2 + \delta_3) \mp \sqrt{(\gamma_2 + i\gamma_3/\omega_a - 2\gamma_1\delta_2 + \delta_3)^2 - 4(-\gamma_1^2 + \gamma_2 + i\gamma_3/\omega_a)(-\delta_2^2 + \delta_3)} \right) \right), \quad (23)$$

where the \mp signs stands for the fast and slow compressional waves respectively. In order to proceed, the source term is set to zero in both Eq. (17) and the domain is restricted to a portion far away from the artificial boundaries so that their contribution can be neglected (Cohen, 2002). Further, it is assumed that the grid is homogeneous and the elements are segments with length h . To perform the discrete dispersion analysis, the basic algebraic equations of a typical degree of freedom must be obtained from Eq. (17) (Zyserman and Gauzellino, 2005). In the present case, it means considering two consecutive elements comprising three nodes, see Fig. 1

Let $u^{s,h}$ and $u^{f,h}$ be expressed in terms of the (local) basis associated with the nodal points in

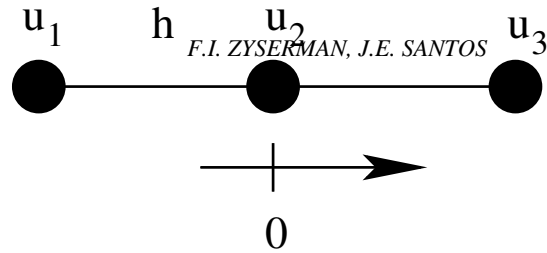


Figure 1: Representative stencil used to derive the numerical dispersion relations. u_i , $i=1,2,3$ are the considered dofs.

Fig.(1) as follows

$$u^{s,h} = \sum_{j=1}^3 \mathbf{u}_j^{s,h} \phi_j(x), \quad (24)$$

$$u^{f,h} = \sum_{j=1}^3 \mathbf{u}_j^{f,h} \phi_j(x). \quad (25)$$

In order to proceed with the dispersion analysis the weak form (17) is tested against the two functions

$$v^s = (\phi_2, 0) \quad v^f = (0, \phi_2), \quad (26)$$

ending up with an homogeneous algebraic system of two equations in 3 unknowns. The coefficients in this system of equations are replaced by standing wave solutions, choosing as the origin of coordinates the central node. Therefore, $u_1 = (u^{s,h}, u^{f,h}) \exp(-iqh)$, $u_2 = (u^{s,h}, u^{f,h})$ and $u_3 = (u^{s,h}, u^{f,h}) \exp(iqh)$. After some algebra a 2×2 the linear system

$$\mathfrak{A} \begin{pmatrix} u_0^{s,h} \\ u_0^{f,h} \end{pmatrix} = 0 \quad (27)$$

is obtained, where

$$\mathfrak{A}_{11} = -2 + 2 \cos(hq^{r,h}) \cosh(hq^{i,h}) + 2i \sin(hq^{r,h}) \sinh(hq^{i,h}) + \left(\frac{h\omega}{3V_R} \right)^2 (2 + \cos(hq^{r,h}) \cosh(hq^{i,h}) + i \sin(hq^{r,h}) \sinh(hq^{i,h})),$$

$$\mathfrak{A}_{12} = -2\delta_2 (-1 + \cos(hq^{r,h}) \cosh(hq^{i,h}) + i \sin(hq^{r,h}) \sinh(hq^{i,h})) + \left(\frac{h\omega}{3V_R} \right)^2 (2 + \cos(hq^{r,h}) \cosh(hq^{i,h}) + i \sin(hq^{r,h}) \sinh(hq^{i,h})) \gamma_1,$$

$$\mathfrak{A}_{21} = \mathfrak{A}_{12},$$

$$\mathfrak{A}_{22} = \delta_3 (-2 + 2 \cos(hq^{r,h}) \cosh(hq^{i,h}) + 2i \sin(hq^{r,h}) \sinh(hq^{i,h})) + \left(\frac{h\omega}{3V_R} \right)^2 ((2 + \cos(hq^{r,h}) \cosh(hq^{i,h}) + i \sin(hq^{r,h}) \sinh(hq^{i,h})) \gamma_2 - \frac{\gamma_3}{3\omega_a} (2i - i \cos(hq^{r,h}) \cosh(hq^{i,h}) + \sin(hq^{r,h}) \sinh(hq^{i,h}))).$$

Forcing this linear system to have nontrivial solutions, i.e., setting

$$\det(\mathbf{A}) = 0, \quad (28)$$

and taking real and imaginary parts, a coupled system of two nonlinear equations in the unknowns $(q^{r,h}, q^{i,h})$ is obtained. Notice that some parameters appear in these equations; they must be fixed beforehand in order to be able to actually get the sought solutions.

The implemented algorithm to obtain $(q^{r,h}, q^{i,h})$ can be described as follows: a) Fix a set of parameters $\delta_i, \gamma_i, i=1,2,3$. b) Fix the number of points per wavelength N_p , c) For each frequency ω_a find h through the relation $h = 2\pi/(N_p q^r)$, where q^r is previously determined from the analytic dispersion relations (See Eq. 23), and solve the nonlinear system by means of a Newton's like method.

5 RESULTS AND DISCUSSION

As already stated, results of the numerical dispersion analysis are shown in terms of dimensionless phase and group velocities and dimensionless attenuation. For the parameters describing the physical properties of the fluid saturated porous medium, the following values were chosen:

$$\delta_1 = \frac{35}{100}, \quad \delta_2 = \frac{8}{100}, \quad \delta_3 = \frac{24}{100}, \quad \gamma_1 = \frac{35}{100}, \quad \gamma_2 = 5, \quad \gamma_3 = \frac{1}{10}, \quad (29)$$

which represent a wide range of water or oil saturated high density sandstones. The set of considered number of points per wavelength was chosen to be $N_p = \{5, 8, 10, 12, 15, 20\}$. From Figures 2, 3 and 4 it can be clearly seen that the fast wave is affected by numerical dispersion; this effect is more noticeable for the phase and group velocities than for the attenuation. In this case, for the normalization factor we have chosen, the relative error can directly be estimated from the pictures, at least for the velocities. It can be noticed that, for example, twelve points per wavelength yield an error of about 1.5% for the phase velocity and almost 2% for the group velocity. These errors can be deemed small in case of working with a computational domain where the wave travels a relatively small number of wavelengths, otherwise, N_p must be increased. Notice that the improvement in the quality of the approximations is not as remarkable as expected when the number of points per wavelength is increased, $N_p=20$ yields an error of about 1.2% for the group velocity. Even though the slow wave behaviour is apparently better, see Figures 5–7, an analysis of the relative error shows that it is not true. Considering the phase velocity and twelve points per wavelength the relative error climbs up to 1.4% for some frequencies, and it is necessary to work with $N_p=15$ to barely keep it less than 1% for all frequencies; the group velocity shows a similar behaviour.

6 CONCLUSIONS

An analysis of the dispersion relations of the Biot equations of motion in the one dimensional cases was presented. The mentioned analysis was carried out by deriving the numerical dispersion relations, and deriving related quantities, such as numerical phase and group velocities and numerical attenuation.

It was observed that all quantities suffer of numerical pollution; therefore, working with a Biot medium using the widespread rule of thumb of ten points per wavelength would lead to rather inaccurate results. At least fifteen points per wavelength must be used in order to guarantee, in

the presently analyzed quantities, a relative error per wavelength less than 1%; a rough upper bound for the error would be the product of this relative error times the number of wavelengths the wave travelled.

7 ACKNOWLEDGMENTS

This work was partially supported by grants PICT 03-13376 (ANPCyT) and PIP 04-5126 (CONICET)

REFERENCES

- J. Bear. Dynamics of fluids in porous media. *Dover Publications, New York*, 1972.
- J. G. Berryman. Confirmation of Biot's theory. *Appl. Phys. Lett.*, 37:382, 1980.
- M. A. Biot. Theory of propagation of elastic waves in a fluid-saturated porous solid. I. Low frequency range. *J. Acoust. Soc. Amer.*, 28:168–171, 1956a.
- M. A. Biot. Theory of propagation of elastic waves in a fluid-saturated porous solid. II. High frequency range. *J. Acoust. Soc. Amer.*, 28:179–191, 1956b.
- M. A. Biot. Mechanics of deformation and acoustic propagation in porous media. *J. Appl. Phys.*, 33:1482–1498, 1962.
- J. M. Carcione. Wave fields in real media: Wave propagation in anisotropic, anelastic and porous media. *Handbook of Geophysical Exploration, Pergamon Press Inc.*, 31, 2001.
- G. Cohen. *Higher-order numerical methods for transient wave equations*. Springer, 2002.
- F. Gassmann. Über die elastizität poröser medien (On the elasticity of porous media). *Vierteljahrsschrift der Naturforschenden Gessellschaft in Zurich*, 96:1–23, 1951. CHE 1856-1999 246.
- J. M. Hovem and G. D. Ingram. Viscous attenuation of sound in saturated sand. *J. Acoust. Soc. Amer.*, 66:1807–1812, 1979.
- D. L. Johnson. Elastodynamics of gels. *Journal of Chemical Physics*, 77(3):1531–1539, 1982.
- D. L. Johnston, J. Koplik, and R. Dashen. Theory of dynamic permeability and tortuosity in fluid-saturated porous media. *J. Fluid Mechanics*, 176:379–402, 1987.
- J. E. Santos, J. M. Corberó, C. L. Ravazzoli, and J. L. Hensley. Reflection and transmission coefficients in fluid-saturated porous media. *J. Acoust. Soc. Amer.*, 91:1911–1923, 1992.
- J. E. Santos, Y. Efendiev, and L. Guarracino. Hydraulic conductivity estimation in partially saturated soils using the adjoint method. Technical Report Series ISC-05-05-MATH, Texas University, 2005.
- A. E. Scheidegger. *The physics of flow through porous media*. University of Toronto, 1974.
- F. Zyserman and P. Gauzellino. Dispersion analysis of a nonconforming finite element method for the three dimensional scalar and elastic wave equations. *Finite elements in analysis and design*, 41:1309–1326, 2005.
- F. I. Zyserman, P. M. Gauzellino, and J. E. Santos. Dispersion analysis of a non-conforming finite element method for the Helmholtz and elastodynamic equations. *Int. J. Numer. Meth. Engng.*, 58:1381–1395, 2003.

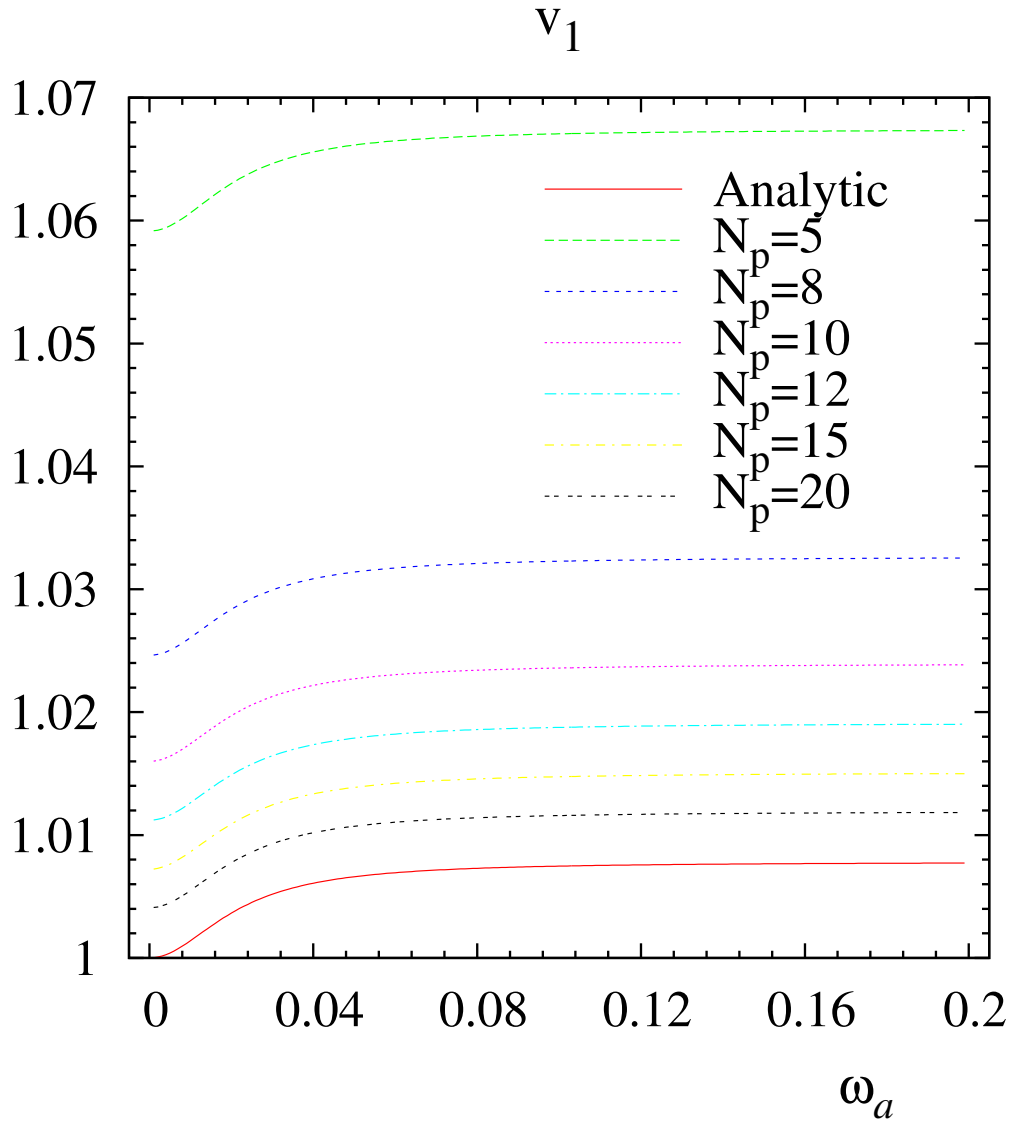


Figure 2: Dimensionless phase velocity for the fast wave P_1 , as a function of the frequency, and for a representative set of N_P .

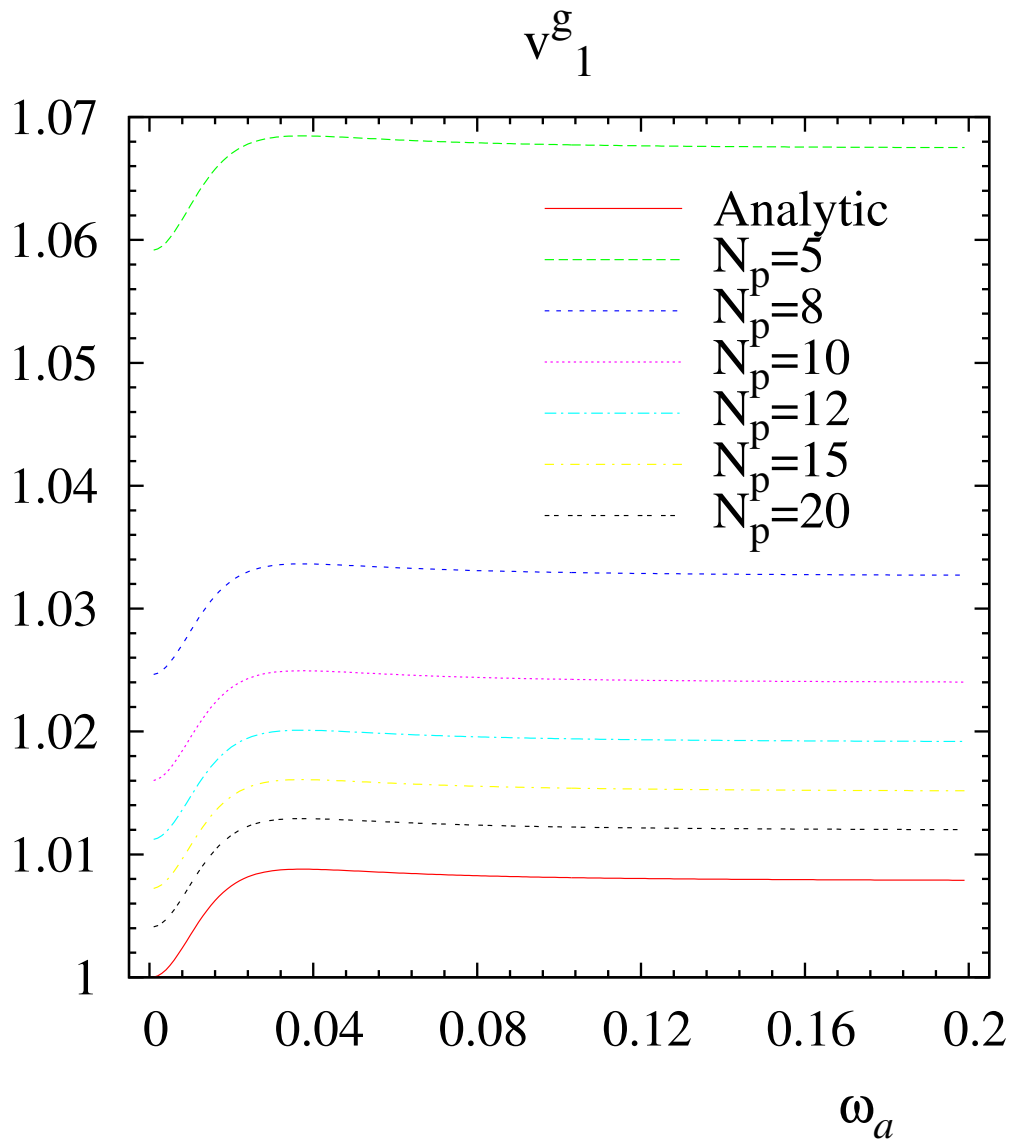


Figure 3: Dimensionless group phase velocity for the fast wave P_1 , as a function of the frequency, and for a representative set of N_p .

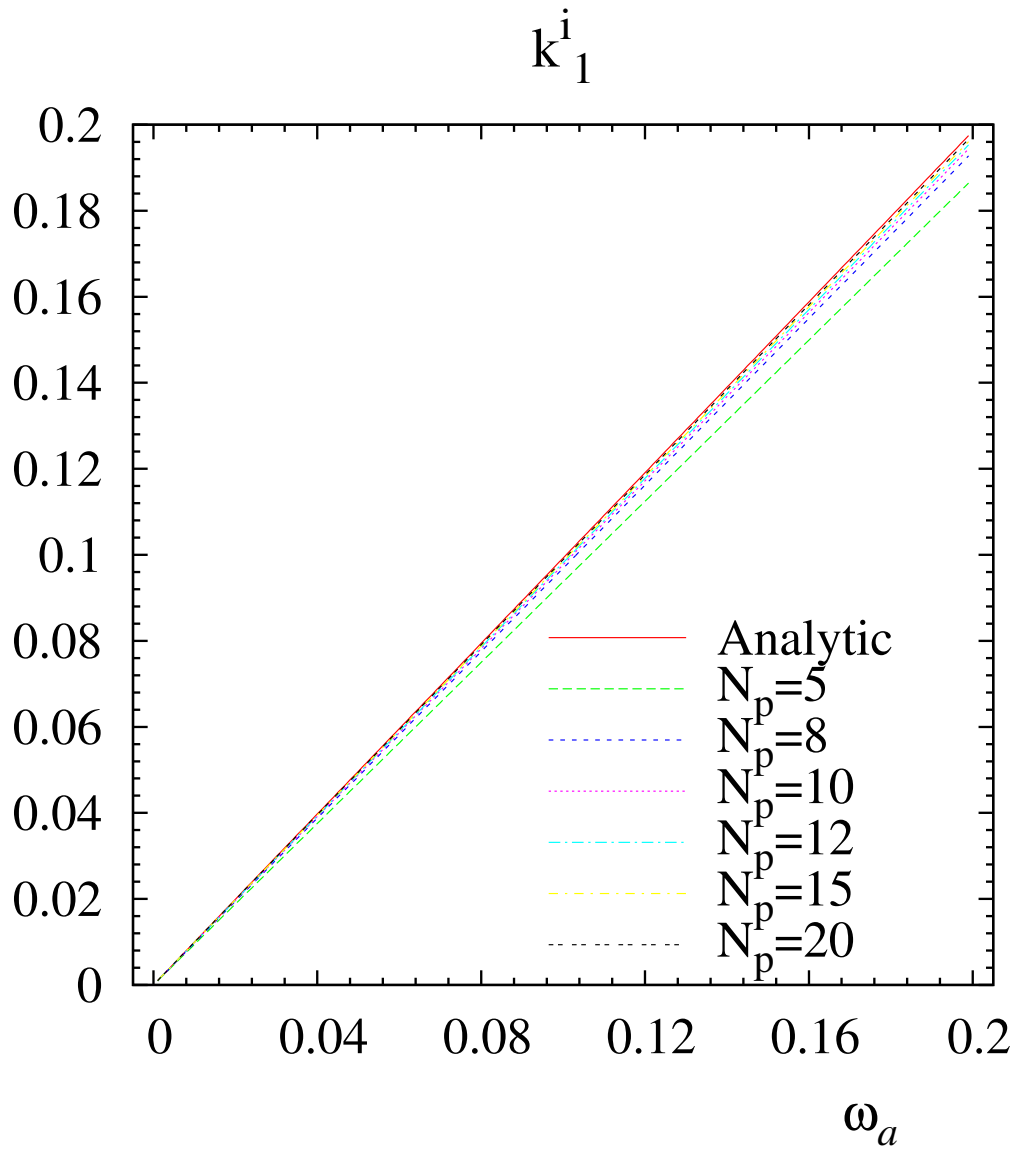
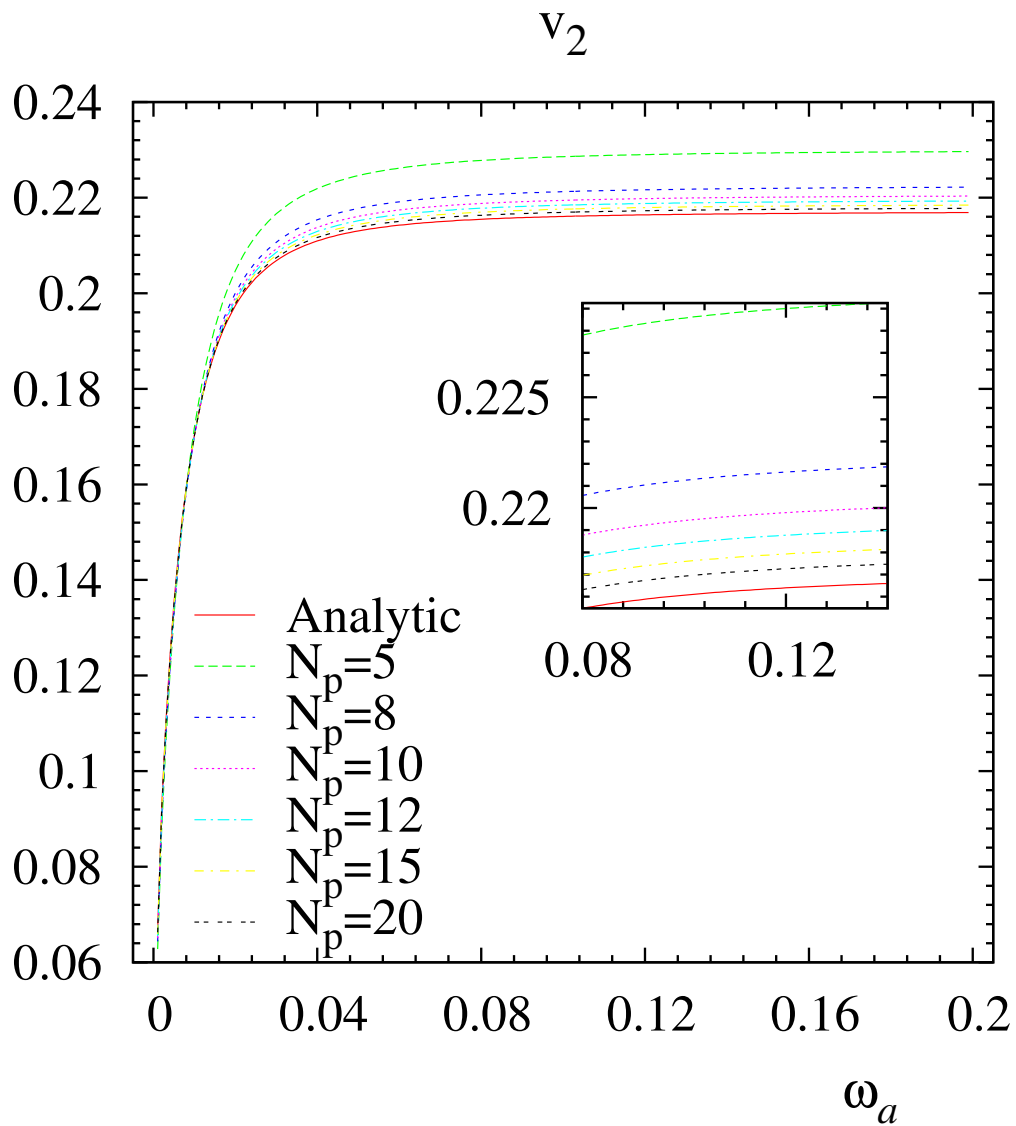


Figure 4: Dimensionless attenuation for the fast wave P_1 , as a function of the frequency, and for a representative set of N_P .

Figure 5: Same as Fig. 2, but for the slow wave P_2 .

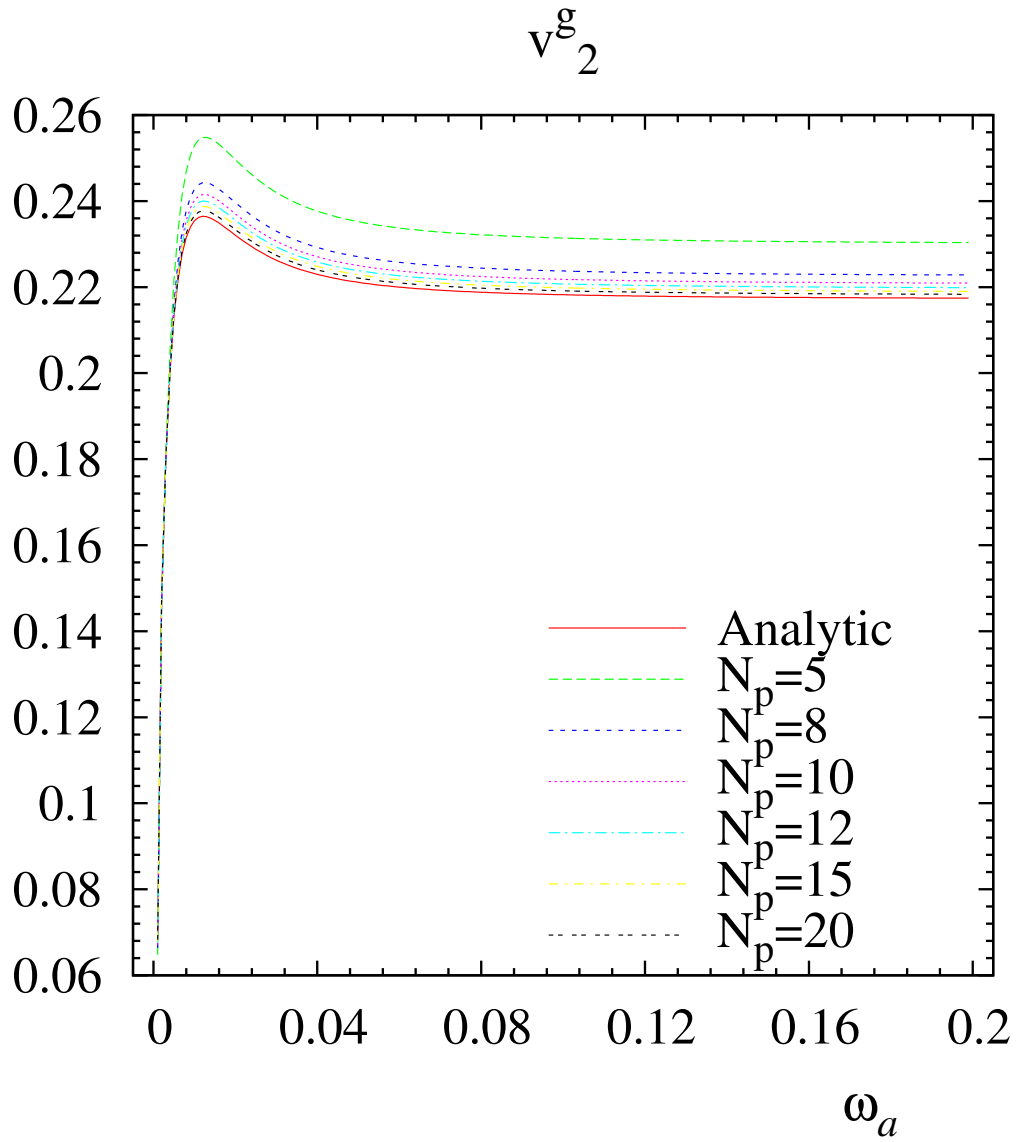
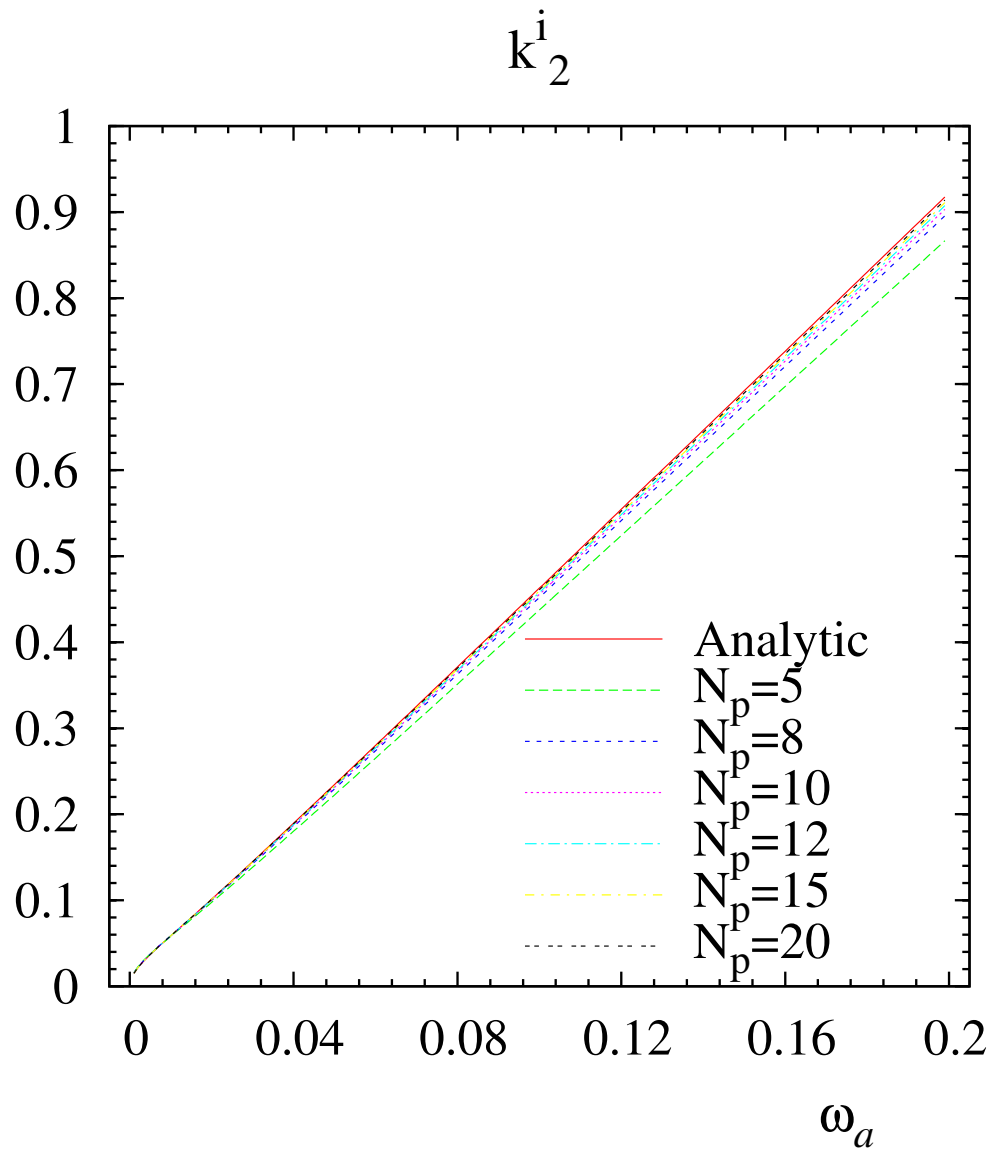


Figure 6: Same as Fig. 3, but for the slow wave P_2 .

Figure 7: Same as Fig. 4, but for the slow wave P_2 .